INTERNATIONAL JOURNAL FOR NUMERICAL METHODS IN FLUIDS, VOL. 3, 295–305 (1983)

A COMPARATIVE STUDY OF CENTRAL AND UPWIND DIFFERENCE SCHEMES USING THE PRIMITIVE VARIABLES

TSAI TIMIN AND M. NABIL ESMAIL

Department of Chemical Engineering, University of Saskatchewan, Saskatoon, Canada S7N 0WO

SUMMARY

The use of the velocity–pressure formulation of the Navier–Stokes equations for the numerical solution of fluid flow problems is favoured for free-surface problems, more involved flow configurations, and three-dimensional flows. Many engineering problems involve such features in addition to strong inertial effects. The computational instabilities arising from central-difference schemes for the convective terms of the governing equations impose serious limitations on the range of Reynolds numbers that can be investigated by the numerical method. Solutions for higher Reynolds numbers $Re > 1000$ could be reached using upwind-difference schemes. A comparative study of both schemes using a method based on the primitive variables is presented. The comparison is made for the model problem of the driven flow in a square cavity. Using a central scheme stable solutions of the pressure and velocity fields were obtained for Reynolds numbers up to 5000. The streamfunction and vorticity fields were calculated from the resulting velocity field and compared with previous solutions. It is concluded that total upwind differencing results in a considerable change in the flow pattern due to the false diffusion. For practical calculations, by a proper choice of a small amount of partial upwind differencing the vorticity diffusion near the walls and the global features of the solutions are not sigificantly altered.

KEY WORDS Primitive Variables Navier–Stokes Central Difference Upwind Difference

INTRODUCTION

A wide scope of engineering problems require reliable solutions for fluid flows in rather complex configurations. In polymer technology and coating processes, fluid flows with free-surfaces and interfaces are commonplace. Strong inertial effects are present in many of the practical problems. All of these factors posed considerable difficulties for the numerical methods used in fluid mechanics. Numerical solutions for the viscous incompressible flow in simply-connected regions have received extensive attention over the last 15 years. Most of the well-established schemes of numerical integration employ the vorticity–streamfunction formulation of the momentum equations. Computer storage economy for two-dimensional calculations and conservation of mass and vorticity for finite spatial intervals seem to be the major advantages of solving the vorticity transport equation. In the case of problems involving free-surfaces and interfaces, the complexity of the boundary conditions, which include the pressure, prohibited the application of the vorticity–streamfunction formulation to an important class of fluid flow problems. In contrast, the pressure–velocity formulation of the Navier–Stokes equations seems more suitable for application of the boundary conditions on free-surfaces and interfaces. Practical problems of an essentially three-dimensional nature posed some difficulties for the vorticity transport equation at intermediate and higher

0271–2091/83/030295–11$01.10

Received 32 August 1981
Revised 8 June 1982

Reynolds numbers, $Re > 400$. Dennis *et al.*[1] argued that three-dimensional schemes for the vorticity transport equation were found to be stable for Reynolds numbers considerably higher than $Re = 100$. However, they cautioned that reliable results need a considerable increase in computer storage requirements and execution time. DeVahl Davis and Mallinson[2] mentioned a three-dimensional solution using a velocity vector potential and vorticity. Although little detail was given in their paper[2] they mentioned solutions limited to $Re \leq 400$. Fasel[3] concluded in his comprehensive review that the Navier–Stokes equations in primitive variable form are easier to extend to three-dimensional problems because of the advantage in computer storage requirements, and the relative simplicity of the boundary condition.

It is well known that the application of finite-difference methods involves a certain compromise in accuracy. Only experimental comparative studies may determine the validity of the approximations used. The desire to extend the numerical solutions to higher Reynolds number applications has been always frustrated by the inherent computational instability of most finite-difference schemes. This instability may be overcome only by the unreasonable tendency towards ever diminishing spatial and temporal intervals of differencing. Compromise techniques such as upwind differencing have received some attention over the last decade. The problems arising from the false diffusion introduced by the first-order approximation have raised a strong wave of objections to the use of upwind differencing. Critical evaluations of this method[4–6] have pointed out some of the advantages and disadvantages, and called for caution.

In the present study a finite-difference approach using the primitive variables is presented. The calculational scheme is based on the Marker and Cell[7,8] intertwined mesh and uses a variable factor of upwind differencing to allow comparative studies of the central scheme and partial upwind differencing. In the study, the recirculating flow in a driven square cavity is selected as a model. The purpose of this work is to examine the possibilities of using central and upwind differencing with the primitive variables formulation, for an intermediate range of Reynolds numbers $Re \geq 1000$. Previous work has been reviewed in a number of papers, for example by DeVahl Davis and Mallinson,[2] Tuann and Olson,[9] and Fasel.[3] The primitive variables approach has been developed by a number of investigators, using the basic ideas of Chorin[8] and Williams.[10] Three-dimensional solutions for the vorticity transport equation have been reported by Dennis *et al.*[1] and Mallinson and DeVahl Davis.[11] Roache's *Computational Fluid Dynamics*,[12] and a recent book by Patankar[13] may also be consulted.

THE MATHEMATICAL MODEL

The recirculating two-dimensional flow of viscous incompressible fluid is governed by the momentum equations. The convective form of these equations may be written as

$$\bar{v}_t + \bar{v} \cdot \nabla \bar{v} = -\nabla p + (1/\mathrm{Re})\nabla^2 \bar{v} + \bar{g}L/U^2 \tag{1}$$

which is known as the Navier–Stokes equation. The Reynolds number is defined as $Re = \rho UL/\mu$, where U is the velocity of the moving wall. The pressure is made dimensionless with respect to ρU^2 and distances—with respect to the side L of the cavity. The conservative form of the Navier–Stokes equation

$$\bar{v}_t + \nabla(\bar{v}; \bar{v}) = -\nabla p + (1/\mathrm{Re})\nabla^2 \bar{v} + \bar{g}L/U^2 \tag{2}$$

is derived from the convective form using the continuity equation

$$\operatorname{div} \bar{v} = 0. \tag{3}$$

Its advantage over the convective form is that it guarantees conservation of momentum for finite spatial intervals of differencing. It has been argued by Bozeman and Dalton[14] that the conservative form yields solutions which are more consistent with the physical problem as defined by Batchelor[15] for large Reynolds numbers. Torrance[6] has shown that the upwind differencing method applied to the conservative equations is considerably more accurate than central differencing applied to the non-conservative equations. The Navier–Stokes equations (1)–(3) in the primitive variables, though satisfying conservation of mass (the continuity equation) in the differential form, do not guarantee this physical law for the discretized equations. Harlow and Welch[7] have shown that non-linear instability may be caused by forcing the dilation to be equal to zero. Instead it is possible according to Chorin[8] to iterate the pressure field in order to satisfy the continuity equation. Harlow and Welch[7] solved a Poisson equation for the pressure with the proper Neumann type boundary conditions. In some applications,[16] the use of non-Neumann type boundary conditions caused fatal deterioration in the convergence of the SOR-iteration.

In our work the solution for the pressure and the velocity components is split by introducing the intertwined mesh system.[8] The flow region is covered with a square perpendicular mesh, which consists of square cells. At the midpoint of each cell side a perpendicular velocity component is prescribed, and the pressure is prescribed at the centre of the cell. An auxiliary velocity field is calculated by the discretized Navier–Stokes equations. The pressure field is determined in the entire flow region and at the boundaries by forcing the dilation D iteratively to satisfy the equation

$$p^{i+1} = p^i - \lambda D,$$
$$D = \frac{\partial u}{\partial x} + \frac{\partial v}{\partial y} \tag{4}$$

where λ is an acceleration parameter determined as $\lambda = 1/2\delta t(1/\delta x^2 + 1/\delta y^2)$. The discretized form of the dilation D is used in equation (4) which is applied to every cell in the mesh. In equation (4), i is the iteration index. Hodge[16] has shown that the pressure iteration (4) can be directly related to an SOR-iteration of a Poisson equation for the pressure. The discretized form of the continuity equation is satisfied by equation (4) by means of varying the pressure, and subsequently adjusting the velocity components in every cell. The simple criterion for stopping the iterations is to require that the continuity is satisfied in every individual cell to a given tolerance.

If X and Y denote the forward displacement operators and X^{-1} and Y^{-1}—the backward displacement operators, the following operators are defined for the x-co-ordinate

$$\delta_x = (X^2 - 1)/2\Delta x \tag{5}$$
$$\bar{\delta}_x = (1 - X^{-2})/2\Delta x \tag{6}$$
$$A_x = (X + X^{-1})/2 \tag{7}$$
$$A_{xx} = (X^2 + 1)/2 = XA_x \tag{8}$$
$$\bar{A}_{xx} = (1 + X^{-2})/2 = X^{-1}A_x \tag{9}$$
$$\delta_{cx} = (X - X^{-1})2\Delta x \tag{10}$$

Similar operators are defined for the y-co-ordinate.

All the spatial derivatives except the convective terms are approximated by a second-order

central difference. For the convective terms we apply the partial upwind differencing[17–19] as follows.

$$\frac{\partial u^2}{\partial x} \simeq (1-w)\delta_{cx}(A_x u)^2 + w[\delta_x(uM^-(\bar{A}_{xx}u) + \bar{\delta}_x(uM^+(A_{xx}u))] \tag{11}$$

$$\frac{\partial uv}{\partial y} \simeq (1-w)\delta_{cy}(A_y uA_y v) + w[\delta_y(uM^-(\bar{A}_{yy}v)) + \bar{A}_{yy}v)) + \bar{\delta}_y(uM^+(A_{yy}v))] \tag{12}$$

$$\frac{\partial uv}{\partial x} \simeq (1-w)\delta_{cx}(A_x uA_x v) + w[\delta_x(vM^-(\bar{A}_{xx}u)) + \bar{\delta}_x(vM^+(A_{xx}u))] \tag{13}$$

$$\frac{\partial v^2}{\partial y} \simeq (1-w)\delta_{cy}(A_y v)^2 + w[\delta_y(vM^-(\bar{A}_{yy}v) + \bar{\delta}_y(vM^+(A_{yy}v))] \tag{14}$$

where

$$M^+(a) = (a+|a|)/2$$
$$M^-(a) = (a-|a|)/2$$
$$X(A_x)^2 = (A_{xx})^2$$
$$X^{-1}(A_x)^2 = (\bar{A}_{xx})^2$$
$$\delta_{cx}(A_x)^2 = [(A_{xx})^2 - (\bar{A}_{xx})^2]/2\Delta x$$

and w is the upwind differencing factor. The time derivative is approximated by a first-order forward difference. The mesh size is $h = 2\Delta x = 2\Delta y$. However, since the velocity components are prescribed at the midpoints of the corresponding cell sides, the finite difference operators are defined for the half-increments Δx and Δy, as the displacement operators are defined for a half step.

The analytical boundary conditions for the velocity are straightforward. No-slip conditions are imposed on three sides of the square, and a tangential constant velocity U is prescribed for the moving wall, with zero normal velocity to ensure that the wall is non-porous. The numerical form of these conditions for the left and right walls is

$$u_w = 0 \qquad \text{at the wall}$$
$$v_{w+\frac{1}{2}} = -v_{w-\frac{1}{2}} \qquad \text{across the wall}$$

For the bottom side the conditions are

$$v_w = 0 \qquad \text{at the wall}$$
$$u_{w+\frac{1}{2}} = -u_{w-\frac{1}{2}} \qquad \text{across the wall}$$

The boundary conditions at the driven wall are

$$v_w = 0 \qquad \text{at the wall}$$
$$u_{w+\frac{1}{2}} = 2U - u_{w-\frac{1}{2}} \qquad \text{across the wall}$$

where the subscript w indicates the wall position. The driven wall condition assumes a linear approximation for the value $u_{w+\frac{1}{2}}$.

RESULTS AND DISCUSSION

The cavity problem as a model has been studied by several investigators. Burggraf[20] reported solutions for Reynolds numbers $Re < 400$. These results were in good agreement with the experimental results of Pan and Acrivos.[21] Other investigators[2,14,22,23] tested novel numerical schemes by solving the model problem. In our study a set of numerical solutions for different Reynolds numbers up to $Re = 5000$ was obtained using various mesh sizes for the central and partial upwind schemes. All solutions were obtained for a cavity with an aspect ratio of one. Three mesh sizes, $h = 2\Delta x = 2\Delta y = 0{\cdot}1$, $0{\cdot}05$ and $0{\cdot}025$, were tested at Reynolds number $Re = 1000$. The three approximations were compared to establish their convergence to a true solution with decreasing mesh size. The vorticity values for the three sizes were compared at the centre of the moving wall, and along the vertical through the centre of the cavity. For the mesh sizes $h = 0{\cdot}1$, $0{\cdot}05$ and $0{\cdot}025$, the vorticity value at the centre of the moving wall was $\zeta = 13{\cdot}3074$, $17{\cdot}9997$, and $18{\cdot}0376$ respectively with a change of about $0{\cdot}2$ per cent when the mesh size was decreased from $h = 0{\cdot}05$ to $h = 0{\cdot}025$. This comparison was made using a central difference scheme $w = 0$. The vorticity along the vertical through the centre of the cavity for $h = 0{\cdot}05$ and $0{\cdot}025$ cannot graphically be distinguished. Subsequently all calculations were made for the mesh size $h = 0{\cdot}025$. The basic output of the calculations consisted of velocity and pressure fields. However, for the purpose of comparison with previous solutions the streamfunction and vorticity were calculated from the final velocity field. The streamfunction $\Psi(x, y)$ defined by the vertical velocity component as

$$v = -\frac{\partial \Psi}{\partial x}$$

may be obtained by discretizing this equation using a central finite-difference representation

$$v_{i-\frac{1}{2},j} h = \Psi_{i-1,j} - \Psi_{i,j}$$

assuming a zero value for the streamfunction at the rigid walls. The vorticity $\zeta(x, u)$ is defined by the equation

$$\zeta = \frac{\partial v}{\partial x} - \frac{\partial u}{\partial y}$$

It may be calculated using the discretized form

$$\zeta_{i,j} = (v_{i+\frac{1}{2},j} - v_{i-\frac{1}{2},j})/h - (u_{i,j+\frac{1}{2}} - u_{i,j-\frac{1}{2}})/h$$

whereas the vorticity boundary values are calculated by a two-dimensional interpolation from the internal values. The convenience of applying central finite-difference formulas for the definitions of the streamfunction and vorticity led to arrays defined at the nodes of the mesh, unlike the velocity and pressure fields. To preserve the stability of calculations, the time step was chosen to ensure that a fluid particle travelled a distance less than the cell size in every cell in the mesh during the time step. For the cases reported in this work $Re = 1000, 2000$ and 5000, the time steps were $5 \times 10^{-5}, 2{\cdot}5 \times 10^{-5}$ and 10^{-5} respectively. The total number of time steps needed to attain steady state ranged from 8,000 to 10,000 in all cases. The pressure iterations within each time step followed one pattern in all cases. In the first time step an average of 120 pressure iterations was needed to adjust the initial data. The number of iterations then subsided rapidly to a minimum of 2–4 pressure iterations in each time step. As mentioned before, our calculations were in the range $1000 \leq Re \leq 5000$.

Although DeVahl Davis and Mallinson[2] computed a case with Re = 5000, they published, like other investigators,[14,23] the data for Re = 1000. Hence, we compare the detail of our results for the same Reynolds number.

Figures 1(a)–(c) illustrate the equivorticity lines for a Reynolds number Re = 1000 for three cases. The first case (Figure 1(a)) is a central difference scheme $w = 0$. The partial upwind schemes (Figures 1(b) and 1(c)) are for $w = 0{\cdot}1$ and $w = 0{\cdot}8$. The core of the primary vortex in Figure 1(a) occupies most of the cavity area and the vorticity is practically constant inside this core. This is consistent with the physical model suggested by Batchelor.[15] Strong vorticity gradients are observed in the neighbourhood of the rigid walls. The corresponding streamlines (Figure 2(a)) show two contrarotating vortices in the lower corners of the cavity

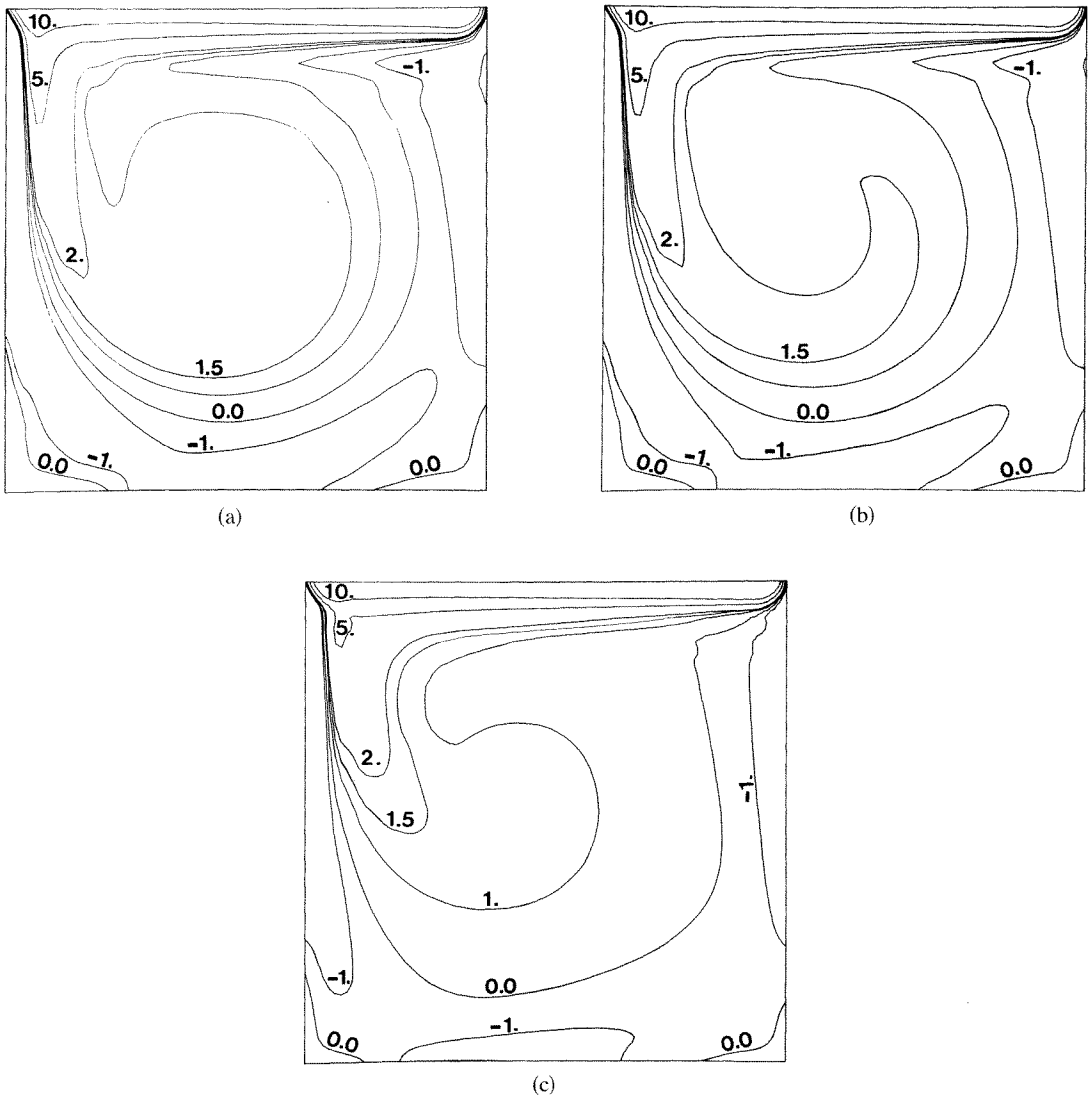

Figure 1. Contour levels for vorticity, Re = 1000. (a) Central scheme $w = 0{\cdot}0$; (b) Partial upwind scheme $w = 0{\cdot}1$, (c) Partial upwind scheme $w = 0{\cdot}8$

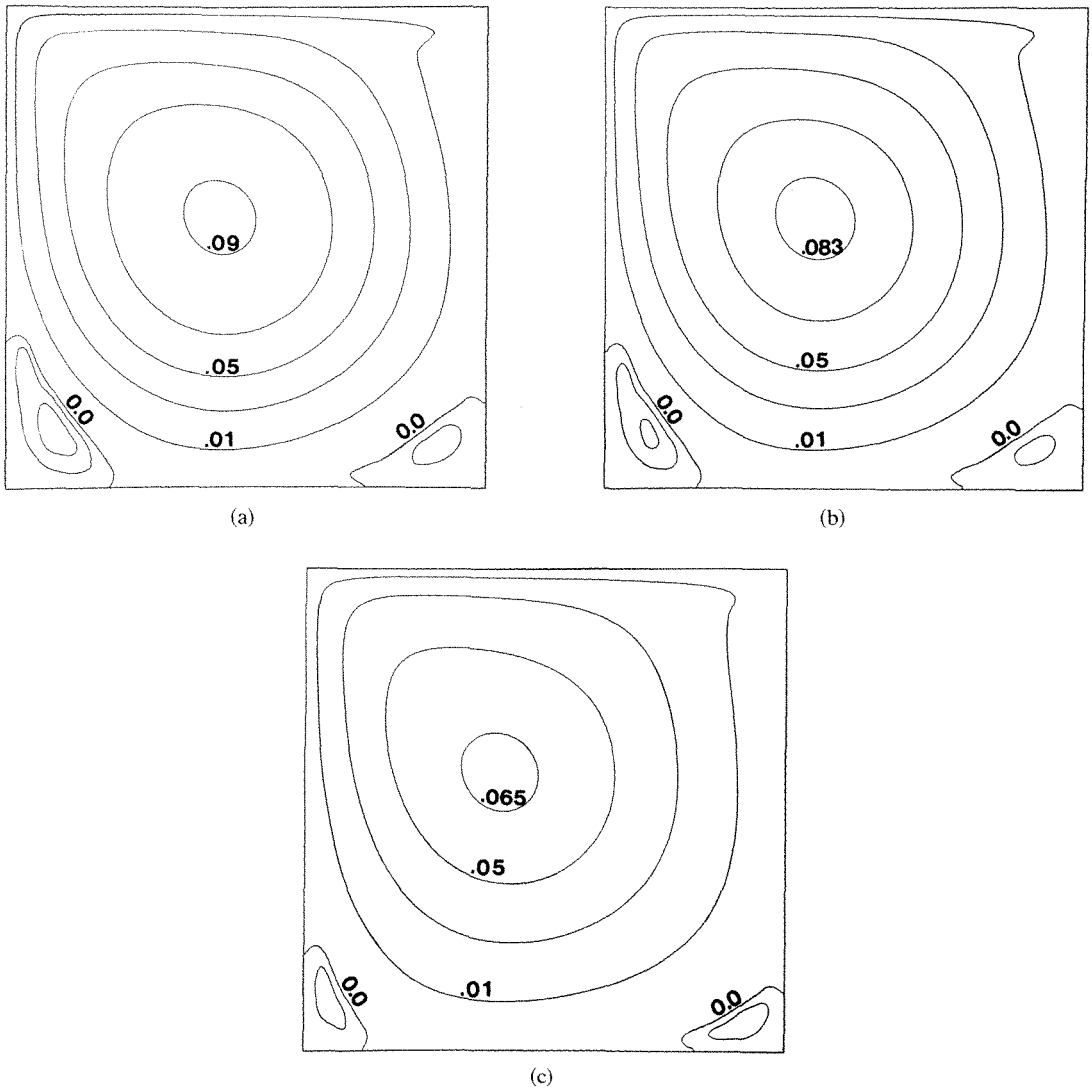

Figure 2. Streamlines, Re = 1000. (a) Central scheme $w = 0{\cdot}0$, (b) Partial upwind scheme $w = 0{\cdot}1$, (c) Partial upwind scheme $w = 0{\cdot}8$

as predicted by most previous work.[2,23] In general, the solution for the central difference scheme (Figures 1(a), 2(a)) is in good agreement with previously accepted solutions, obtained for the vorticity–streamfunction formulation, using an implicit iterative method.[2] In the coarser mesh $h = 0{\cdot}1$, the central difference scheme converged to a solution with an oscillatory nature in the vorticity values near the moving wall. In contrast, with a strong partial upwind component $w = 0{\cdot}8$ (Figure 1(c)) the vorticity gradients near the rigid walls are reduced, and the primary vortex core is smaller. This is an indication of a lower Reynolds number solution. The corner vortices are smaller in size compared to the results of the central scheme, as illustrated by the streamlines (Figures 2(a), 2(c)). Although the formal first-order accuracy $o(\Delta x)$ of the upwind differencing scheme[12] retains 'something' of the

second-order accuracy of the advection field, if the dependent variable is slowly varying in space (nearly linear advection), for intermediate Reynolds numbers (e.g. Re = 1000) the solution is seriously afflicted by the false diffusion. Such features were observed in previous work.[2,23] Our calculations with a small partial upwind component $w = 0{\cdot}1$ (Figures 1(b), 2(b)) show that the global features of the vorticity diffusion (Figure 1(b)) remain close to the second-order solution of the central difference scheme. Since the streamfunction is a less sensitive value, it may be observed in Figures 2(a) and 2(b) that the streamlines for $w = 0$ and $w = 0{\cdot}1$ are almost identical. The corner vortices are of the same size in both solutions and are in good agreement with previous vorticity transport solutions.[2] The streamlines of the upwind scheme $w = 0{\cdot}8$ (Figure 2(c)) are noticeably different from other solutions, and the

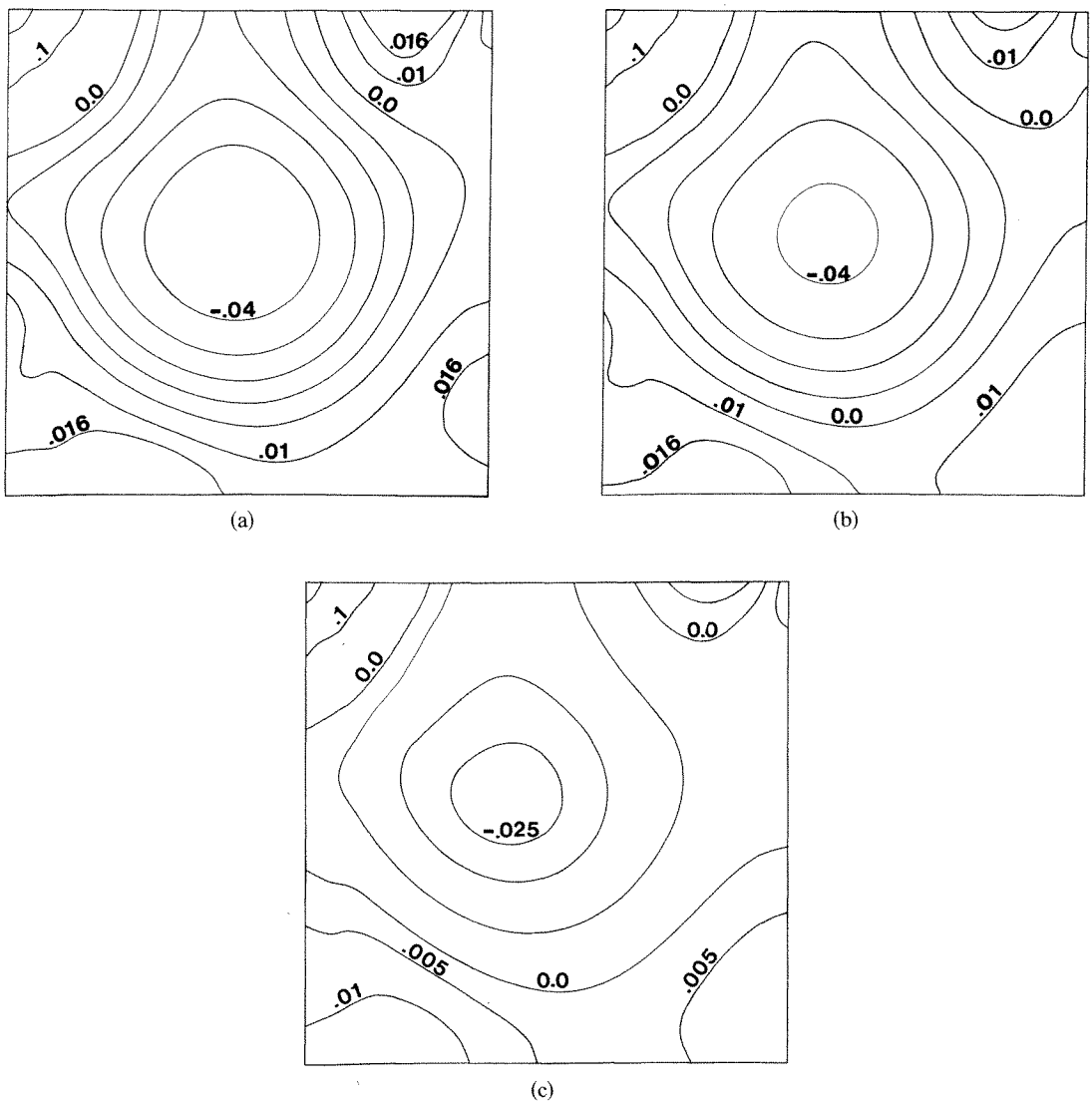

Figure 3. Contour levels for pressure, Re = 1000. (a) Central Scheme $w = 0{\cdot}0$, (b) Partial upwind scheme $w = 0{\cdot}1$, (c) Partial upwind scheme $w = 0{\cdot}8$

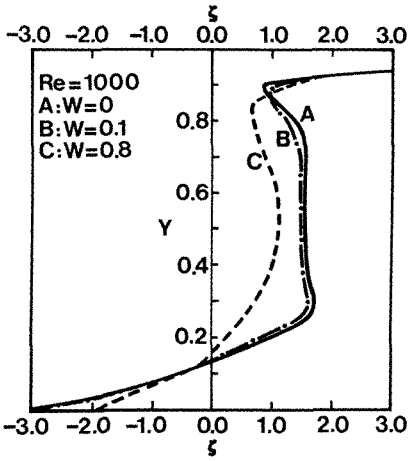

Figure 4. Vorticity distribution along a line through the centre of the primary vortex

corner contrarotating vortices are smaller. The pressure contours for Re = 1000, using the same difference schemes, are shown in Figures 3(a)–(c). The core of the cavity is a negative pressure region. The pressure gradients near the rigid walls are greatest in the case of the central difference scheme (Figure 3(a)). The contours experience noticeable changes as we increase the upwind component to $w = 0{\cdot}1$ and then $w = 0{\cdot}8$ (Figures 3(b), 3(c)). One more measure of examining the numerical solutions is to compare the vorticity distribution along a line through the centre of the primary vortex. This comparison (Figure 4) shows that the small partial upwind-difference component $w = 0{\cdot}1$ slightly deflects the values obtained by the central scheme. The strong upwind scheme $w = 0{\cdot}8$ considerably influences the rate of vorticity transport to the core of the cavity. The comparison with previous work[2,14] indicates that the central difference scheme yields solutions in agreement with the physical features of the problem. Upwind difference schemes seem to lead to progressively inaccurate results as

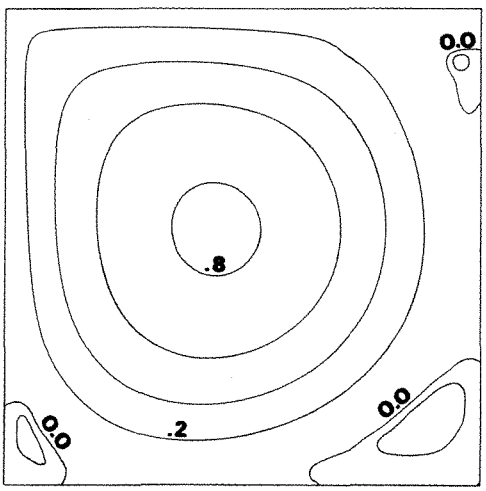

Figure 5. Streamlines, Re = 2000, $w = 0{\cdot}0$, central scheme

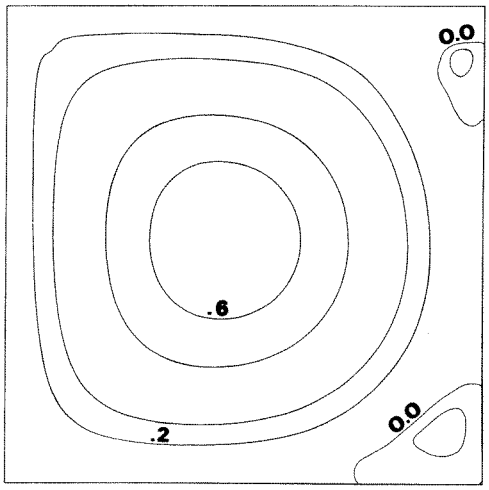

Figure 6. Streamlines, Re = 5000, $w = 0{\cdot}0$, central scheme

the upwind component w is increased. The pressure and vorticity are more sensitive to the false diffusion introduced by the first-order approximation of the advection terms in upwind differencing.

The central difference scheme $w = 0$ produced stable solutions with the mesh size $h = 0{\cdot}025$ up to a Reynolds number of Re = 5000 (Figures 5 and 6). In these figures the values of the streamfunction are multiplied by a factor of 10. A third, secondary vortex appears downstream near the moving wall at a Reynolds number Re = 2000 (Figure 5), and the constant vorticity core is enlarged (Figure 6) as expected with higher Reynolds numbers. The oscillatory behaviour of the vorticity observed by Keller[24] for Re = 5000 and $h = 0{\cdot}01$ is not present in our calculations for the same Reynolds number using the central difference scheme and $h = 0{\cdot}025$. Calculations for higher Reynolds number (Re = 10,000) were attempted. With a time step of $\Delta t = 10^{-5}$ and a mesh size $h = 0{\cdot}025$ the calculations suffered from persistent oscillations, and wiggles appeared in the streamlines. A smaller time step would probably cure these symptoms, since the global features of a larger constant vorticity core and the continuation of the secondary vortices pattern observed for Re = 5000 were present. It is our conclusion that for the intermediate range of Reynolds numbers, the use of central difference scheme for the convection terms leads to more reliable results. Upwind differencing schemes show considerable changes in the solution, especially in the vorticity and pressure fields.

REFERENCES

1. S. C. R. Dennis, D. B. Ingham and R. N. Cook, 'Finite-difference methods for calculating steady incompressible flows in three dimensions', *J. Comp. Phys.*, **33,** 325–339 (1977).
2. G. DeVahl Davis and G. D. Mallinson, 'An evaluation of upwind and central difference approximations by a study of recirculating flow', *Comp. Fluids*, **4,** 29–43 (1976).
3. H. Fasel, *Computational Fluid Dynamics*, Hemisphere, New York, 1980, pp. 167–279.
4. G. D. Raithby, 'A critical evaluation of upstream differencing applied to problems involving fluid flow', *Comp. Meth. Appl. Mech. Eng.*, **9,** 75–103 (1976).
5. P. J. Roache, 'On artificial viscosity', *J. Comp. Phys.*, **10,** 169–184 (1972).
6. K. Torrance, 'Comparison of finite difference computations of natural convection', *J. Res. N.B.S.*, **72B,** 281–301 (1968).

7. F. H. Harlow and J. E. Welch, 'Numerical calculation of time-dependent viscous incompressible flow of fluid with free-surface', *Phys. Fluids*, **8,** 2182–2189 (1965).
8. A. J. Chorin, 'Numerical solution of the incompressible Navier–Stokes equations', *Math. Comp.*, **22,** 745 (1968).
9. S. Y. Tuann and M. D. Olson, 'Review of computing methods for recirculating flows', *J. Comp. Phys.*, **29,** 1–19 (1978).
10. G. P. Williams, 'Numerical integration of the three-dimensional Navier–Stokes equations for incompressible flow, *J. Fluid Mech.*, **37,** 727–750 (1969).
11. G. D. Mallinson and G. DeVahl Davis, 'The method of the false transient for the solution of coupled elliptic equations', *J. Comp. Phys.*, **12,** 435 (1973).
12. P. J. Roache, *Computational Fluid Dynamics*, Hermosa, Albuquerque, New Mexico, 1972.
13. S. V. Patankar, *Numerical Heat Transfer and Fluid Flow*, Hemisphere, New York, 1980.
14. J. D. Bozeman and C. Dalton, 'Numerical study of viscous flow in a cavity', *J. Comp. Phys.*, **12,** 348–363 (1973).
15. G. K. Batchelor, 'On steady laminar flow with closed streamlines at large Reynolds numbers', *J. Fluid. Mech.*, **1,** 177–190 (1956).
16. J. K. Hodge, 'Numerical solution of incompressible laminar flow about arbitrary bodies in body-fitted curvilinear coordinates', *Ph.D. Thesis*, Mississippi State University, 1975.
17. D. B. Spalding, 'A novel finite difference formulation for differential expressions involving both first and second derivatives', *Int. J. num. Meth. Engng*, **4,** 551–559 (1972).
18. G. D. Raithby and K. E. Torrance, 'Upstream-weighted schemes and their application to elliptic problems involving fluid flow', *Comp. Fluids*, **2,** 191–206 (1974).
19. F. H. Harlow and A. A. Amsden, 'A numerical fluid dynamic calculation method for all flow speeds', *J. Comp. Phys.*, **8,** 197–213 (1971).
20. O. R. Burggraf, 'Ananytical and numerical studies of the structure of steady separated flows', *J. Fluid Mech.*, **24,** 113–152 (1966).
21. F. Pan and A. Acrivos, 'Steady flows in rectangular cavities', *J. Fluid Mech.*, **28,** 643–655 (1967).
22. R. D. Mills, 'Numerical solutions of the viscous flow equations in a class of closed flows', *J. Roy. Aero. Soc.*, **69,** 714–718 (1965).
23. A. D. Gosman, W. M. Pun, A. K. Runchal, D. B. Spalding and M. Wolfstein, *Heat and Mass Transfer in Recirculating Flows*, Academic Press, London, 1969.
24. H. B. Keller, 'Bifurcation and limit point calculations in some viscous flow problems', *Proc. 2nd Int. Conf. Computational Methods in Nonlinear Mechanics*, Univ. of Texas, Austin (1979).